

A Study of Commonsense Reasoning over Visual Object Properties

Abhishek Kolari[†] Mohammadhossein Khojasteh[†] Yifan Jiang[◊] Floris den Hengst[†] Filip Ilievski[†]

[†]Department of Computer Science, Vrije Universiteit Amsterdam, Netherlands

[◊]Information Sciences Institute, University of Southern California, Marina del Rey, CA, USA

abkolari08@gmail.com

{m.khojasteh, f.den.hengst, f.ilievski}@vu.nl, yifjia@isi.edu

Abstract

Inspired by human categorization, object property reasoning involves identifying and recognizing low-level details and higher-level abstractions. While current visual question answering (VQA) studies consider multiple object properties, such as size, they typically blend perception and reasoning and lack representativeness in terms of reasoning and image categories, making it unclear whether and how vision-language models (VLMs) abstract and reason over depicted objects. To this end, we introduce a systematic evaluation framework comprising images of three representative types, three reasoning levels of increasing complexity, and four object property dimensions, informed by prior work on common sense. We develop a procedure to instantiate this framework in two VQA object reasoning benchmarks: OPTICS-CNT, comprising 360 images paired with 1,080 multi-level, count-based questions, and OPTICS-CMP, with 2.1k comparison questions. Experiments with 12 state-of-the-art VLMs in zero-shot settings reveal significant limitations relative to humans, with the best-performing model achieving below 40% counting and 70% comparison accuracy. VLMs struggle particularly with photographic images, counterfactual reasoning, physical and functional properties, and higher counts. We make the OPTICS benchmark data and code available to support future work on scalable benchmarking methods, generalized annotation guidelines, and advanced reasoning VLMs.

1 Introduction

Object representation and reasoning is one of the core systems of human cognition (Spelke and Kinzler, 2007). By abstracting object properties and interactions, humans, including infants

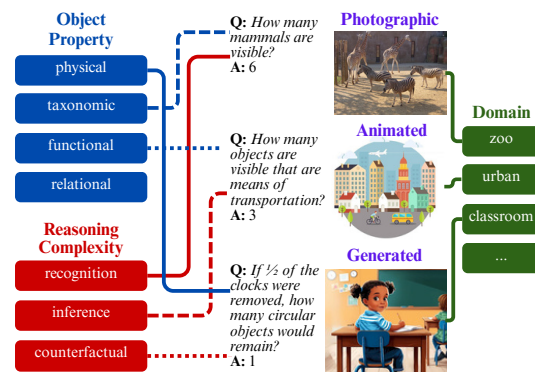


Figure 1: VQA in **OPTICS-CNT**, with questions about different **object properties** of varying **reasoning complexity** on three **types of images** from different **domains**.

with limited real-world knowledge and experience, represent their environment and perform inference (Lipton and Spelke, 2004). Object representation and reasoning in humans are driven by spatio-temporal principles of cohesion (objects move as connected, bounded wholes), continuity (objects move along connected, unobstructed paths), and contact (objects do not interact at a distance). Humans perceive object boundaries, represent object shapes that move (partially) out of view, and predict object movement (Aguiar and Baillargeon, 1999; Leslie and Keeble, 1987). Importantly, object perception and inference is not merely descriptive; it involves a multi-stage process from low-level recognition, through categorization, to identification and reasoning (Fields, 2016). For instance, to count how many mammals are visible in Figure 1-top, humans recognize the image objects, decide which of them fit the constraint (type) of a mammal, and count those.

Recent work on the connection between perception and reasoning has used visual question answering (VQA) in natural language as a diagnostic task for vision-language models (VLMs). Existing VQA benchmarks evaluate recognition of

Category		VQAv2	CLEVR	TallyQA	SCIENCEQA	GQA	C-VQA	CFMM	OPTICS
Question	Counting Comparison	✓	✓	✓	✓	✓	✓	✓	✓
Object Property	Physical Taxonomic Functional Relational	✓	✓	✓	✓	✓	✓	✓	✓
Image Type	Real Animated AI-Generated	✓	✓	✓	✓	✓	✓	✓	✓
Reasoning	Direct Recognition Property Inference Counterfactual	✓	✓	✓	✓	✓	✓	✓	✓

Table 1: Comparison of **OPTICS** to closely related existing benchmarks: VQAv2 (Goyal et al., 2017), CLEVR (Johnson et al., 2017), TallyQA (Acharya et al., 2018), SCIENCEQA (Lu et al., 2022), GQA (Hudson and Manning, 2019), C-VQA (Zhang et al., 2024b), and CFMM (Li et al., 2024).

basic visual elements such as physical attributes or taxonomic category membership (Yuan et al., 2021; Tong et al., 2024), inference of relational properties (Lu et al., 2022; Hudson and Manning, 2019), and counterfactual reasoning (Frohberg and Binder, 2021; Yu et al., 2023; Li et al., 2024). As objects are central components of images, solving these benchmarks relies on extracting and reasoning over physical and abstract object properties (Johnson et al., 2017; Hudson and Manning, 2019; Acharya et al., 2018).

Current VQA evaluation exhibits two key limitations. The first is the *lack of a delineation between subtasks for object perception and reasoning*, i.e., object detection, inference, and counterfactual reasoning. While some studies have identified small object sizes and peripheral locations as causes of failure in VLMs (Zhang et al., 2025, 2024a), the lack of subtask separation hinders comprehensive diagnosis of their strengths and weaknesses. Second, we note a *limited representativeness of the covered evaluation dimensions*, usually focusing on basic features such as shape and color (Goyal et al., 2017; Antol et al., 2015). Jiang et al. (2024)’s recent systematic evaluation of abstract visual reasoning covers different types, configurations, and shapes. Given its focus on manipulating simple shapes in synthetic environments with minimal noise, the ability of VLMs to perceive and reason over real-world objects across image types remains underexplored.

We address this gap in the understanding of the capabilities of current models with a *compre-*

hensive, fine-grained evaluation of the ability of VLMs to perceive and reason given a representative range of object properties, reasoning complexities, and image types. We make three contributions (Figure 1): 1. **A systematic evaluation framework** for object property reasoning, consisting of three image types, three levels of reasoning complexity, and four dimensions of commonsense knowledge. 2. **A semi-automatic procedure** for dataset creation, resulting in two VQA benchmarks based on our framework: **OPTICS-CNT** with 1.1k high-quality counting questions about 360 images, and **OPTICS-CMP** with 2.1k comparison questions about image pairs.¹ 3. **An extensive experimental analysis** of state-of-the-art (SotA) VLMs on OPTICS, revealing fine-grained limitations of current models for photographic images, counterfactual reasoning, functional knowledge, and higher counts.

2 Related Work

Object Properties in VQA. VQA has long served as a diagnostic task for evaluating the perceptual and reasoning capabilities of AI systems. Early efforts (Antol et al., 2015; Goyal et al., 2017) emphasized general visual recognition of objects, colors, and basic attributes, while subsequent benchmarks (Singh et al., 2019; Mathew et al., 2021; Lu et al., 2022) targeted domain-specific context. Although many benchmarks across domains (Johnson et al., 2017; Hudson and Man-

¹OPTICS stands for Object Property Reasoning Tasks for Evaluating Image-based Common Sense.

ning, 2019; Acharya et al., 2018) require reasoning over object properties, none of them provides a systematic separation of object property dimensions. Compared to previous VQA benchmarks, our framework covers four distinct object dimensions based on commonsense resources (Speer et al., 2017; Ilievski et al., 2021; Kurtz and Silliman, 2021): physical, taxonomic, functional, and relational, and enables fine-grained assessment of object-level reasoning as visualized in Table 1. Moreover, while both counting and comparison questions have been relatively well-covered in prior work, our evaluation enables compositional evaluation by comparing counts across images rather than object properties (e.g., which object is larger (Li et al., 2024)).

Visual Reasoning Complexity. Human cognition is inherently compositional and integrates multiple scene aspects into higher-level reasoning, with complexity progressing from direct recognition to property-level inference, and counterfactual reasoning (Hoffman and Richards, 1987; Xu et al., 2021). Initial *direct recognition* is limited to recognition of basic visual elements such as physical attributes or taxonomic category membership (Yuan et al., 2021; Tong et al., 2024). *Inference* builds on recognition, targets higher-level functional or relational properties, and requires multi-step abstraction beyond surface-level features (Lu et al., 2022; Hudson and Manning, 2019). *Counterfactual reasoning* involves reasoning about hypothetical changes made in inputs. This type of reasoning is most challenging, as it requires understanding and adapting to hypothetical, altered, or out-of-context scenarios (Frohberg and Binder, 2021; Yu et al., 2023; Li et al., 2024). Benchmarks that target different types of reasoning exist (Table 1), yet none systematically test reasoning levels simultaneously. Inspired by compositional evaluation frameworks in abstract visual reasoning (Jiang et al., 2024), OPTICS is the first to encompass all three reasoning types and go beyond previous work to study VLM performance across three image types, thereby enabling a more comprehensive assessment of models’ perception and reasoning abilities. To support fair evaluation, we focus on counting and comparison questions in line with prior benchmarks (Acharya et al., 2018; Johnson et al., 2017; Li et al., 2024).

3 A Commonsense Framework for Evaluating Object Property Reasoning

We devise a systematic framework for rigorous evaluation of VLMs, integrating *object property dimensions* (physical, taxonomic, functional, relational), *levels of reasoning complexity* (recognition, property inference, counterfactual), and diverse *image types* (photographic, animated, AI-generated). We next detail its three components.

3.1 Object Property Dimensions

Drawing on prior research (Ilievski et al., 2021; Tandon et al., 2017) on representing commonsense knowledge about properties and their relations, our framework distinguishes four object property dimensions relevant for counting and comparison VQA. Each dimension captures a distinct facet of human conceptualization and reasoning about object attributes and relations in visual scenes.

Physical knowledge refers to the dynamics of physical systems based on observable phenomena and fundamental principles (McCloskey et al., 1983) (e.g., *circular objects* in Figure 1). Physical properties, such as object qualities, materials, and part-whole relations, are prevalent in commonsense knowledge representation (Tandon et al., 2017; Fleming, 2017). Our framework enhances the list of physical properties in prior VQA studies, such as shape, color, and size (Table 1), with more complex attributes like the *material* (wood, metal), *state* of the object (liquid, solid), and structural characteristics of the object – including part-whole relationships such as *has wheels*.

Taxonomic knowledge captures an object’s semantic category or class membership, typically expressed as *is-a* relations (Ilievski et al., 2021). Examples in our framework include broad ontological groupings, e.g., *biological* (e.g., mammals, reptiles), *artifact* (e.g., furniture, tools), and *food* (e.g., fruits, vegetables) categories. Unlike physical attributes, taxonomic properties may not be visible from visual input alone: to determine how many mammals are present in an image (Figure 1), visual identification of species must be combined with knowledge of their taxonomic classification. The taxonomic dimension aligns with *taxonomic semantic systems* from cognitive science and domain-specific knowledge representation, which group entities based on shared features and categorical similarity (Mirman et al., 2017).

Functional properties express attributes such as

utilities and *capabilities* of an object (e.g., means of transportation in Figure 1), *affordances* as actions an object receives (e.g., breakable, foldable), and *operational dependencies* for an object to function (e.g., electricity, battery). This dimension primarily aligns with the *utility* and *causal* relations identified in commonsense knowledge frameworks (Speer et al., 2017; Heindorf et al., 2020; Ilievski et al., 2021). Questions about the utility of objects have been included in VQA studies (Table 1): for example, the OK-VQA benchmark (Marino et al., 2019) tests for knowledge about object utility, e.g., *a broom is for sweeping*. **Relational** knowledge captures how objects interact, how they can be contextually grouped, and how they are situated relative to each other within a visual context. Attributes include *spatial relationships* (as in *"How many objects can be seen hanging from the wall?"*) and *contextual grouping relations* (as in *"How many couples are visible?"*), inspired by commonsense knowledge organization (Ilievski et al., 2021). Its emphasis on relations between multiple object instances complements the focus on properties of single objects in taxonomic and part-whole physical properties.

3.2 Reasoning Complexity

The four object property dimensions can support questions with varying reasoning complexity. Our three levels of reasoning complexity: *direct recognition*, *property inference*, and *counterfactual reasoning* are exemplified in Figure 1. We expect that the progression from direct recognition to counterfactual reasoning requires an increasingly high level of abstraction to answer a question, and a shifting emphasis from perception to reasoning, thus increasing in difficulty (Xu et al., 2021).

Direct Recognition questions ask about features that can be detected by observation and general categorical knowledge. Questions at this level can be answered through an atomic step of perception and reside at the physical and taxonomic property dimensions. For example, the top question in Figure 1 only requires identifying land animals and categorizing them as mammals.

Property Inference questions target the functional and relational property dimensions, which require deeper abstraction, introducing multi-step reasoning. It studies the ability of models to generalize beyond surface-level features by focusing on codependencies among objects and underlying

relations across different image regions. For example, in Figure 1, the middle question requires identifying a bicycle, a car, and a plane, categorizing them as vehicles, and then reasoning about their utility in transportation.

Counterfactual Reasoning questions probe the ability to reason about hypothetical, altered, or out-of-context scenarios. Counterfactual questions span any of the four property dimensions. In addition to visual recognition and inference, counterfactual questions also require commonsense knowledge and flexible abstraction (e.g., creating a contextualized procedure that identifies remaining circular objects besides half of the clocks in the bottom question of Figure 1), thus forming the most complex reasoning level in our framework.

3.3 Image Types

To study VLM generalization across visual domains, we cover various image types, expecting that accuracy varies (often worsens) when moving from synthetic to real-world images (Johnson et al., 2017; Hudson and Manning, 2019).

Photographic images represent naturalistic settings, featuring complex textures, lighting variations, and cluttered scenes. They are realistic, i.e., all depicted objects are found in the real world. Photographs present challenges such as occlusions, viewpoint variation, and natural ambiguity, requiring an effective visual grounding.

Animated images are simplified or stylized and contain minimal visual noise, as well as limited levels of detail when compared to photographic images. Humans typically create animated images in digital form, and their objects are not necessarily realistic. Object boundaries in animated images may be easier to detect, but exaggerated representations may pose a novel challenge.

AI-generated images include both photorealistic and stylized images, created by prompting generative models. They test robustness to domain shifts by deviating from visual conventions such as real-world physics and object proportions. AI-generated images typically feature simpler compositions and include implausible objects, such as half-animals or floating glasses.

4 Benchmark Construction

Our dataset curation follows a four-phase pipeline (Figure 2). We *collect images* from public sources corresponding to the three image types. Then, we

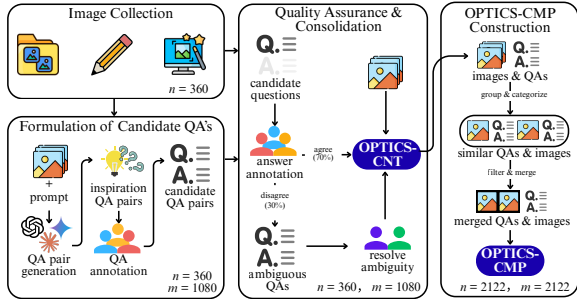


Figure 2: OPTICS-CNT and OPTICS-CMP construction pipeline: image collection, candidate QA formulation, quality assurance, and pairwise combination. n and m are number of images and QAs, respectively.

ask an annotator to *formulate candidate question-answer* pairs for all images, inspired by AI-generated questions. Then, the questions and answers undergo additional rounds of human refinement for *quality assurance*, which results in OPTICS-CNT. OPTICS-CMP is then *systematically constructed* from samples in OPTICS-CNT. Finally, we present statistics about the two benchmarks. We detail each step below.

Image Collection. To ensure diagnostic quality and mitigate data contamination risks from existing benchmarks (Dodge et al., 2021), we collect previously unsourced images. We define 26 domains grouped into three categories based on the MacGyver dataset (Tian et al., 2025) (see Table 6 for details). We use these domains as queries across all three image types, enabling fair comparisons of images from comparable scenes. We collect public images by querying a variety of sources: Google Images, Unsplash, and Freepik for photographic and animated images; GPT-4o and Grok3 for AI-generated ones (see Table 5 for example generative AI prompts). We explicitly exclude diagrammatic images (Lu et al., 2022). In total, we collect 360 images (120 per type).

Formulation of Candidate QA-pairs. We formulate initial question-answer pairs using a semi-automatic procedure. Namely, we prompt a multimodal large-language model (MLLM) to generate three counting questions (one per reasoning level) following the framework defined in the previous section. The MLLM is selected at random from GPT-4o (OpenAI et al., 2024), Claude 3.7 Sonnet (Anthropic, 2025), and Gemini 2.0 Flash (Google et al., 2025a). The resulting 1,080 question-answer pairs are then used by five human annotators, who are instructed to revise or replace

them to ensure high quality. Namely, humans ensure that the question is precise and fits the restrictions of our evaluation framework, and that the answer count is not too high (we cap the answers at 10). Each of the annotators is responsible for 72 images. When possible, the annotators are instructed to abstract over the specific object types, e.g., prioritizing “how many objects are made of rubber?” over “how many tires are made of rubber?”. In practice, the annotators rewrote a vast majority of the questions and nearly all answers, as many MLLM-generated questions were ambiguous or repetitive, and most answers were incorrect.

Quality Assurance and Consolidation of OPTICS-CNT. Human annotators may introduce controversial assumptions and biases. To ensure a broader consensus and catch ambiguous questions, we perform two rounds of quality assurance. First, each of the 360 images is randomly assigned to an annotator (from the same pool) who did not annotate the QA pair in the previous phase. This annotator is provided with the question and the image, and asked to provide an answer. Comparing the two annotators’ answers for each question, we observed that they agreed on 756 answers (70%). We identified two key disagreement sources: 1) Semantic ambiguity: Uncertainty in the definition, including objects that partially satisfy a property (e.g., a knife that is partly metal) or objects with unclear definitions (e.g., a container). 2) Visual ambiguity: Uncertainty in the visual information, such as deciding whether to count a partially visible chair. We addressed these disagreements by another round of quality assurance, where a third, different annotator looked at the question, answer, and comments and attempted to resolve the disagreement by rephrasing the questions to make them more precise, or if that was challenging, to replace them with a new QA pair from the same reasoning complexity level. This results in OPTICS-CNT.

Construction of OPTICS-CMP. To introduce an evaluation axis beyond exact counting and diversify question types, we devise OPTICS-CMP, which assesses the ability to make *relative* judgments between images. OPTICS-CMP is derived from annotated VQA samples in OPTICS-CNT. We first group questions by object properties and reasoning complexity, then pair them using semantic similarity (Reimers and Gurevych, 2019). For each pair, the corresponding images are re-

Let A be the answer to *left question* for the *left image*. Let B be the answer to *right question* for the *right image*. Which is greater, A or B ?

Figure 3: OPTICS-CMP question template.

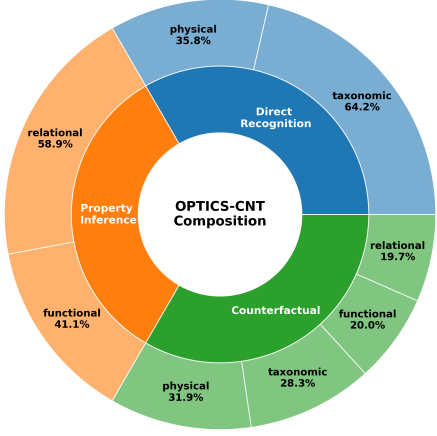


Figure 4: OPTICS-CNT question composition.

sized and concatenated. Then, a comparison question is generated using the template in Figure 3, and an answer is automatically derived from the OPTICS-CNT labels (see example in Figure 9).

Benchmark Composition and Analysis. OPTICS-CNT integrates the images, questions, and final ground truth answers in a dataset containing 1,080 questions about 360 high-quality images of photographic, animated, and AI-generated types in equal proportions. The overall distribution across object properties is also relatively balanced (Figure 4). We observe a larger portion of taxonomic over physical questions in the direct recognition category, and similarly, slightly more relational than functional questions in the inference category. Curiously, when creating counterfactual questions, annotators prioritized physical and taxonomic over relational and functional knowledge. Meanwhile, OPTICS-CMP comprises 2,122 comparison questions created from merged image pairs, where the count difference spans from 1 to 9. Notably, 80% of the comparisons fall within a difference of 1–4. The most common question pairs in OPTICS-CMP involve direct recognition of an object’s taxonomic (56.7%) or physical (22.1%) properties (details in Figure 10). We also estimated the OPTICS-CNT difficulty

for humans by asking two new participants to answer 90 questions about 30 random images from OPTICS-CNT, split across reasoning levels and object properties. Their overall accuracy of 74% indicates that while the task is challenging for humans, they answer most questions correctly.

5 Experimental Setup

Model Selection. To ensure representative evaluation, we include a variety of non-instruction-tuned and instruction-tuned open-source VLMs, as well as a fine-tuned VLM and a closed-source model. As non-instruction-tuned open-source VLMs, we include BLIP-2 (Li et al., 2023) combined with OPT-2.7b and OPT-6.7b (Zhang et al., 2022), and Fuyu-8b (Bavishi et al., 2023). We include the instruction-tuned open-source models BLIP-2 paired with Flan T5-xxl (Chung et al., 2024), Qwen2.5-VL (3B, 7B, and 32B Instruct models) (Bai et al., 2025), and InternVL3 family (8B and 14B variants) (Zhu et al., 2025) prominent on the Hugging Face OpenVLM Leaderboard (Duan et al., 2024), and Gemma 3 (Google et al., 2025b) with 27B parameters. Our study incorporates the SpatialVLM fine-tuned version of Qwen2.5-VL for spatial relations and depth estimation in VQA (Chen et al., 2024), SpaceThinker-Qwen2.5-VL, claimed by the authors to be their most accurate fine-tuned specialized reasoning model. As a closed-source VLM, we include only GPT-4o-mini due to budget considerations (OpenAI et al., 2024). All models are evaluated in a zero-shot setting using standard hyperparameters.

Answer Extraction. For both benchmarks, our VLM prompts facilitate answer extraction by requesting either the total count or a count followed by objects for OPTICS-CNT (see Table 4), and only “A” or “B” to indicate which value is greater for OPTICS-CMP. To extract answers from OPTICS-CNT (numeric label) and OPTICS-CMP (A or B label), we employ flexible regular expressions for detection and perform exact string matching against ground-truth labels. For OPTICS-CNT, we interpret missing outputs as a prediction of zero, and though during data curation we restrict object counts to 10 per image, we allow model outputs with counts greater than 10 to enable analysis of deviation from ground truth.

Evaluation Metrics. Following established count-based VQA benchmarks (Trott et al., 2018; Acharya et al., 2018), we report multiple eval-

Model	Micro Acc (↑)	Macro Acc (↑)	RMSE (↓)	Mean Error (→ 0)	Off- By- 1 (↑)
<i>Random</i>	9.09	9.09	4.47	0.00	25.62
BLIP-2 OPT (2.7B)	12.87 [†]	10.92	3.66	-2.68	35.28
BLIP-2 OPT (6.7B)	16.67 [†]	9.68	3.06	-1.56	46.11
Fuyu (8B)	19.91	11.88	2.68	-0.89	49.72
BLIP-2 Flan (11B)	15.93 [†]	12.95	3.53	-2.05	42.59
Qwen2.5 (3B)	24.91	23.55	15.30	-1.16	51.85
Qwen2.5 (7B)	38.70	<u>31.57</u>	<u>1.88</u>	-0.62	70.28
Qwen2.5 (32B)	39.91	34.46	1.80	-0.35	72.78
SpaceThinker (3B)	29.63	25.32	2.19	-0.89	62.50
InternVL3 (8B)	37.59	31.30	1.93	-0.70	70.28
InternVL3 (14B)	39.72	29.90	2.08	-0.91	68.61
Gemma3 (27B)	31.76	24.43	2.20	-0.14	65.28
GPT-4o mini	30.37	22.74	15.19	-0.36	64.17
<i>Model average</i>	28.16	22.39	4.62	-1.02	58.28
<i>Human 1</i>	75.56	75.15	4.22	0.64	82.22
<i>Human 2</i>	72.22	67.27	1.63	-0.24	85.56
<i>Human average</i>	73.89	71.21	2.92	0.2	83.89

Table 2: Zero-shot results on OPTICS-CNT. The highest and second-highest model results are highlighted in **bold** and underlined, respectively. (↑)/(↓) indicates that higher/lower values are better. (→ 0) signifies values closer to zero are better. [†] means the result is attributed to inductive bias.

uation metrics for OPTICS-CNT. Our primary measure is *micro accuracy (Acc)*. We report *macro accuracy*, which averages the accuracy scores across different counts, ranging from 0 to 10. We also report *Root-Mean-Squared Error (RMSE)* to quantify the typical deviation between predicted and ground-truth counts. To diagnose model bias, we include *mean error*, which reveals bias towards over- or under-counting. Furthermore, *off-by-N* accuracy (cumulative accuracy by tolerance) indicates the proximity of the predictions to the correct count. We also report accuracy per count difference for OPTICS-CMP, expecting an increase in accuracy for larger differences.

6 Results

How well can VLMs accurately count and reason about object properties? The results for OPTICS-CNT in Table 2 show that *most models perform above random, but well below human accuracy (28% versus 74% on average)*. The high RMSE across many of the models indicates substantial variance in predictions, suggesting that

precise numerical grounding is challenging, even for strong VLMs. The negative mean error values suggest consistent underestimation and a general bias towards undercounting. We note a severely imbalanced prediction distribution in the outputs of some VLMs (detailed in Figure 14). When allowing for one counting error, the accuracy increases to 58% on average (to 73% for the best model), which indicates that many model errors are near-misses (see Figure 15 for an in-depth analysis of the top-3 best performing VLMs). For all VLMs, the micro accuracy is higher than the macro accuracy because all models exhibit a bias towards lower, more frequent counts, as shown in Figure 5. In contrast, human accuracy is uniform across answer counts, with no apparent frequency bias. We further analyze the sources of errors for both humans and VLMs at the end of this section.

How does counting performance vary across VLMs? Accuracies vary widely across models, ranging from 12.87% to 39.91%. The open-source Qwen2.5-VL-Instruct (32B) is the best-performing model, with the highest exact and off-by-1 accuracies, the lowest RMSE, and the lowest mean error. A small gap separates it from InternVL3 (14B), with the second-highest overall accuracy, and Gemma 3 (27B), which achieves the lowest mean error. The closed-source GPT-4o-mini exhibits moderate performance, with a high RMSE and low mean error. We also note a typical increase in performance with increasing model size within model families, though this may not always hold across architectures. Table 3 shows that Qwen2.5-VL-Instruct (7B) and (32B) demonstrate the strongest performance across nearly all reasoning levels, property dimensions, and image types, while GPT-4o-mini performs consistently worse than most instruction-tuned open-source models.

How does counting performance vary across reasoning levels? We expect the progression of reasoning complexity *recognition* < *property inference* < *counterfactual* (§3) to be reflected in corresponding trends in model performance. However, the results among the top-tier VLMs (Qwen2.5-VL-Instruct, InternVL3, Gemma 3, and GPT-4o-mini) reveal a progression *property inference* < *recognition* < *counterfactual*. This suggests that modern VLMs still exhibit poor low-level perceptual capabilities, which aligns with several recent findings: 1) Jiang et al. (2024) showed poor perceptual performance of MLLMs

Model	Reasoning Complexity			Object Properties				Image Types		
	Direct Recognition	Property Inference	Counter-factual	P	T	F	R	Photo	Animated	AI Gen.
BLIP-2 OPT (2.7B)	10.83	13.06	14.72	11.48	14.41	10.91	13.78	9.17	19.44	10.00
BLIP-2 OPT (6.7B)	16.67	18.06	15.28	16.39	16.52	14.09	19.08	14.17	21.11	14.72
Fuyu (8B)	18.33	22.78	18.61	17.21	17.42	19.55	25.44	16.94	23.89	18.89
BLIP-2 Flan (11B)	18.33	18.61	10.83	14.34	16.82	13.64	18.02	11.67	20.00	16.11
Qwen2.5 (3B)	26.11	29.17	19.44	21.31	29.43	17.73	28.27	20.28	27.78	26.67
Qwen2.5 (7B)	42.78	44.17	29.17	35.66	42.34	32.73	<u>41.70</u>	32.22	40.83	43.06
Qwen2.5 (32B)	<u>39.17</u>	<u>43.06</u>	37.50	<u>33.61</u>	<u>44.44</u>	38.18	41.34	<u>31.94</u>	<u>45.00</u>	<u>42.78</u>
SpaceThinker (3B)	34.44	30.28	24.17	25.00	37.24	19.55	32.51	25.56	31.11	32.22
InternVL3 (8B)	38.89	41.94	31.94	33.20	42.34	26.82	44.17	28.89	43.61	40.28
InternVL3 (14B)	42.78	42.22	<u>34.17</u>	30.33	48.05	<u>36.82</u>	40.28	32.22	48.61	38.33
Gemma3 (27B)	33.89	35.56	25.83	26.23	34.53	28.64	35.69	27.78	36.39	31.11
GPT-4o mini	28.89	33.61	28.61	21.31	34.23	25.00	37.81	24.44	38.89	27.78
<i>Model average</i>	29.34	31.04	24.18	23.83	31.48	23.63	31.50	22.94	33.05	28.49
<i>Human 1</i>	73.33	80.00	73.33	58.33	92.00	71.43	80.00	63.33	83.33	80.00
<i>Human 2</i>	66.67	76.67	73.33	58.33	80.00	76.19	75.00	60.00	83.33	73.33
<i>Human average</i>	70.00	78.33	73.33	58.33	86.00	73.81	77.50	61.66	83.33	76.66

Table 3: Accuracy results for each model on OPTICS-CNT across reasoning levels, object property dimensions (Physical, Taxonomic, Functional, Relational), and image types. The highest and second highest model results are highlighted in **bold** and underlined, respectively.

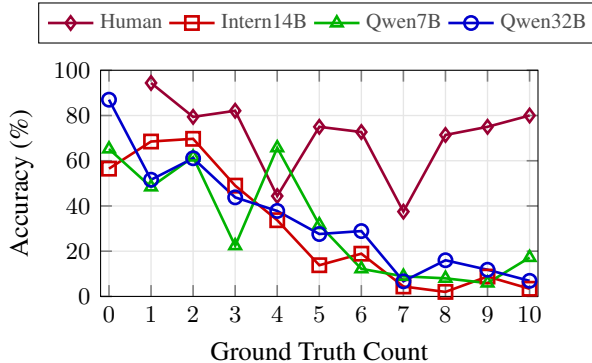


Figure 5: Accuracy per count (0-10) for human with an average (micro) accuracy of 73.89% and the top-3 best performing models: Qwen2.5-VL-Instruct (32B), InternVL3 (14B), and Qwen2.5-VL-Instruct (7B).

for fine-grained visual analysis tasks, including counting; 2) [Zhang et al. \(2024a\)](#) identified blind spots in MLLMs, including sensitivity to visual quality and image distractors; 3) [Yuan et al. \(2021\)](#) showed perception failures in the MetaVQA framework and highlighted the need for detailed perceptual grounding of VLMs. The lower accuracy on counterfactual questions is indicative of difficulty with changes and hypotheticals, reliance on learned associations, and lack of reliable grounding ([Li et al., 2024](#)). Humans also perform best on inference questions, but struggle

less than VLMs with counterfactual reasoning.

How does counting accuracy vary across object properties?

Among the object property dimensions, most models (as well as humans) have a stronger grasp of taxonomic and relational questions than of physical and functional ones. This finding is in line with recent work that points out the struggle of LLMs with physical object attributes ([Wang et al., 2023](#)), physical interactions ([Aroca-Ouellette et al., 2021](#)), functional requirements ([Qasemi et al., 2022](#)), and atypical affordances ([Tian et al., 2025](#)). We note an improvement for the fine-tuned SpaceThinker-Qwen2.5-VL (3B) model compared to its non-fine-tuned counterpart, Qwen2.5-VL (3B), across the four object property dimensions. This shows that, in addition to relational questions, other object properties also benefit from spatial tuning of Qwen2.5 (3B). We also observe that the InternVL3 models have a better grasp of taxonomic and relational questions compared to other models. The Qwen2.5-VL (7B) and (32B) variants demonstrate consistent performance across all properties, with particular strength in physical and functional questions. In contrast, the non-instruction-tuned models struggle across all properties, underscoring their weakness in visual object reasoning.

How does counting performance vary across image types? We observe a consistently higher accuracy for AI-generated and animated images, compared to photographic images. We hypothesize that this is due to the visually cleaner, less cluttered nature of AI-generated and animated images compared to the complex, noisy real-world scenes in photographic images. This finding aligns with previous studies reporting similar gaps between synthetic and real-world data (Johnson et al., 2017; Hudson and Manning, 2019). Moreover, we note that animated images are easier for most models than AI-generated images, possibly because the latter may have poor focus and include implausible objects, such as a half-cut glass floating in the air. The trend between the image difficulty *animated* < *AI-generated* < *photographic* is also clear in humans, which indicates that questions about photographic images may be the hardest and possibly contain remaining ambiguity.

How well do VLMs answer comparison questions, and is this sensitive to the count differences? Based on results from OPTICS-CNT, we evaluate only the instruction-tuned models on OPTICS-CMP. This experiment confirms that VLMs struggle with counting objects, even in this relative setting. Namely, VLMs’ accuracy remains only slightly higher than random, at 58% (details in Table 9). Qwen2.5-VL (32B) remains the overall best-performing model, followed by InternVL3 (8B), which outperforms its larger (14B) variant. This pattern does not hold within the Qwen2.5-VL family, where we instead observe a steady increase in performance as model size increases. Our hypothesis that VLMs would show higher gains on larger count differences is examined in Figure 6. While some models clearly follow this trend, we note that the model performance across the count differences remains broadly stable. These findings confirm those from the absolute-counting task but also demonstrate that the failure modes of humans and VLMs may differ. We next dive deeper into the causes for errors in both humans and VLMs.

How similarly do humans and VLMs make mistakes? To investigate this, we selected 25 questions for which both the best VLM (Qwen2.5-VL-32b) and at least one human judge gave an incorrect answer relative to the ground truth. We defined four categories of errors: 1) *Semantic ambiguity* errors caused by unclear semantic constraints in the question, e.g., should an object that

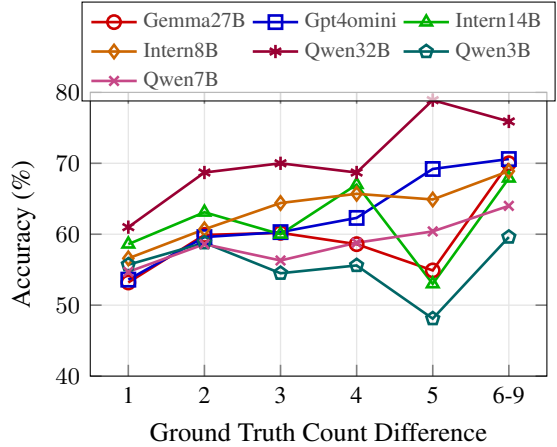


Figure 6: Accuracy per count difference (1-9) for instruction-tuned VLMs on OPTICS-CMP. Counts (6-9) are grouped as one.

is half wood and half metal be counted as “metal”? 2) *Visual ambiguity* errors caused by ambiguous visual information in the image, e.g., should we count a chair if only part of its legs is visible and not the whole object? 3) *Perception errors* - honest mistakes due to overlooking or misperceiving information, e.g., not noticing a small object or miscounting the number of items. 4) *Unnatural errors* that are highly unlikely for a human to make, e.g., counting a glass as a metal object or counting an object that clearly does not exist.

We assigned each incorrect answer from the model and the human judge to one or more of these four categories. We observe the following (full results in Table 10): a) Humans do not make unnatural mistakes (0/25), whereas the model makes many of them (9/25). This is the most significant difference between humans and the model, which may stem from hallucination/illusion-driven errors in models, as evidenced by diagnostic suites (Guan et al., 2024). An example is shown in Figure 7 (right), where the human counted all objects that could be considered metal, while the model counted items like the glass and the cutting board, which are clearly not metal. b) For humans, the majority of mistakes (16/25) come from semantic ambiguity, not knowing whether something should be counted or how to interpret a specific condition. This finding is consistent with our analysis of image types, which concluded that photographic images may be most challenging due to remaining ambiguity in the questions or in the visual content. c) The second most common source of human error is per-

	Question: If one turtle slid off the log into the water, how many turtles would be in the water?
	Correct Answer: 2
	Human's Answer: 1 [turtle]
	Model's Answer: 1 [turtle]
	Question: If there were twice as many knives in the image, how many metal objects would be shown in total?
	Correct Answer: 8
	Human's Answer: 10 [6 knives, 1 pot, 1 tap, 2 cooking spots]
	Model's Answer: 6 [knives, pot, glass, stove burner, faucet, cutting board]

Figure 7: Examples of errors made by humans and the model. **Left:** Both the model and the human made a perception error. **Right:** The human made a semantic ambiguity error, while the model made an unnatural error.

ception errors (9/25), often due to not examining the image carefully enough and missing objects. Perception errors are similarly frequent in humans and the model (9 and 8, respectively). An example is shown in Figure 7 (left), where both the human and the model made the same mistake: they missed the turtle inside the water.

7 Conclusions

This paper developed a commonsense evaluation framework for evaluating object property reasoning in images. The framework considered three distinct image types (photographic, animated, and AI-generated), three reasoning levels (direct recognition, property inference, counterfactual), and four property types (physical, taxonomic, functional, relational). We instantiated this framework on two VQA benchmarks: OPTICS-CNT, with over 1,000 counting questions across 360 images, and OPTICS-CMP, with over 2,000 comparison questions across as many images. Experiments with 12 state-of-the-art VLMs revealed low counting accuracy, with most models performing far below human performance and the best achieving only 40% accuracy. VLMs struggle particularly with realistic (photographic) images, counterfactual reasoning about physical and functional properties, and infrequent counts over five. Humans also struggle with photographic images and physical properties but excel at counterfactual questions and have no frequency effects on counts. Interestingly, when asked to compare images based on their counts, most VLMs performed better for higher differences, but their performance on very large differences remained relatively modest. Analyzing closely the errors made by humans and VLMs revealed that, while both make a sizeable proportion of perceptual mistakes, VLMs are dominated by unnatural errors, whereas humans

struggle with semantic ambiguity. This indicates that VLMs experience limitations on a combination of perception and reasoning abilities and unexpected hallucinations.

Future work should address three emerging limitations. First, generative AI still suffers from limited accuracy and diversity in autonomous question generation, causing *scaling up object reasoning benchmarks to require substantial human effort*. Our attempt to generate a scalable version based on richly annotated data (§B.5) showed that automatically creating such benchmarks remains challenging. Novel approaches, such as metamorphic testing (Yuan et al., 2021), are necessary to grow OPTICS-CNT systematically in size and coverage of additional object properties, question types beyond counting and comparison, and open-ended answers. Second, since annotators are free to design their own questions, they may *introduce semantic ambiguity*, leading to disagreements (e.g., whether zebras are considered black animals). Although we addressed ambiguity through an explicit quality assurance step that analyzes sources of disagreement and translates them into more precise guidelines, some disagreements remain. Future work should develop generalizable and well-understood guidelines for object abstraction and reasoning. Finally, while OPTICS-CNT and OPTICS-CMP point to fundamental limitations of popular and diverse VLMs, *the set of baselines is inherently incomplete*. Future work should explore additional specialized reasoners beyond SpatialVLM, e.g., a referring expression counting method to address compositional attribute filters and counting (Dai et al., 2024), mixtures of experts (Lin et al., 2024), derivation of object schemas (Hsu et al., 2024), and methods for populating situational scene graphs following predefined slots (Sugandhika et al., 2025).

References

Manoj Acharya, Kushal Kafle, and Christopher Kanan. 2018. [Tallyqa: Answering complex counting questions](#).

Andréa Aguiar and Renée Baillargeon. 1999. 2.5-month-old infants’ reasoning about when objects should and should not be occluded. *Cognitive psychology*, 39(2):116–157.

Anthropic. 2025. [Claude 3.7 sonnet and claude code](#). *Anthropic News*.

Stanislaw Antol, Aishwarya Agrawal, Jiasen Lu, Margaret Mitchell, Dhruv Batra, C Lawrence Zitnick, and Devi Parikh. 2015. Vqa: Visual question answering. In *Proceedings of the IEEE international conference on computer vision*, pages 2425–2433.

Stéphane Aroca-Ouellette, Cory Paik, Alessandro Roncone, and Katharina Kann. 2021. Prost: Physical reasoning of objects through space and time. *arXiv preprint arXiv:2106.03634*.

Shuai Bai, Keqin Chen, Xuejing Liu, Jialin Wang, Wenbin Ge, Sibo Song, Kai Dang, Peng Wang, Shijie Wang, Jun Tang, Humen Zhong, Yuanzhi Zhu, Mingkun Yang, Zhaohai Li, Jianqiang Wan, Pengfei Wang, Wei Ding, Zheren Fu, Yiheng Xu, Jiabo Ye, Xi Zhang, Tianbao Xie, Zesen Cheng, Hang Zhang, Zhibo Yang, Haiyang Xu, and Junyang Lin. 2025. Qwen2.5-vl technical report. *arXiv preprint arXiv:2502.13923*.

Rohan Bavishi, Erich Elsen, Curtis Hawthorne, Maxwell Nye, Augustus Odena, Arushi Soman, and Sagnak Tasirlar. 2023. Fuyu-8b: A multimodal architecture for ai agents. *URL: https://www.adept.ai/blog/fuyu-8b*.

Boyuan Chen, Zhuo Xu, Sean Kirmani, Brain Ichter, Dorsa Sadigh, Leonidas Guibas, and Fei Xia. 2024. Spatialvlm: Endowing vision-language models with spatial reasoning capabilities. In *Proceedings of the IEEE/CVF Conference on Computer Vision and Pattern Recognition (CVPR)*, pages 14455–14465.

Hyung Won Chung, Le Hou, Shayne Longpre, Barret Zoph, Yi Tay, William Fedus, Yunxuan Li, Xuezhi Wang, Mostafa Dehghani, Siddhartha Brahma, et al. 2024. Scaling instruction-finetuned language models. *Journal of Machine Learning Research*, 25(70):1–53.

Siyang Dai, Jun Liu, and Ngai-Man Cheung. 2024. Referring expression counting. In *Proceedings of the IEEE/CVF Conference on Computer Vision and Pattern Recognition*, pages 16985–16995.

Jesse Dodge, Maarten Sap, Ana Marasović, William Agnew, Gabriel Ilharco, Dirk Groeneweld, Margaret Mitchell, and Matt Gardner. 2021. Documenting large webtext corpora: A case study on the colossal clean crawled corpus. *arXiv preprint arXiv:2104.08758*.

Haodong Duan, Junming Yang, Yuxuan Qiao, Xinyu Fang, Lin Chen, Yuan Liu, Xiaoyi Dong, Yuhang Zang, Pan Zhang, Jiaqi Wang, et al. 2024. Vlmevalkit: An open-source toolkit for evaluating large multi-modality models. In *Proceedings of the 32nd ACM International Conference on Multimedia*, pages 11198–11201.

Chris Fields. 2016. How humans recognize objects: Segmentation, categorization and individual identification.

Roland W Fleming. 2017. Material perception. *Annual review of vision science*, 3(1):365–388.

Jörg Frohberg and Frank Binder. 2021. Crass: A novel data set and benchmark to test counterfactual reasoning of large language models. *arXiv preprint arXiv:2112.11941*.

Google, Gemini Team, Rohan Anil, Sebastian Borgeaud, Jean-Baptiste Alayrac, Jiahui Yu, Radu Soricut, Johan Schalkwyk, Andrew M Dai, Anja Hauth, Katie Millican, et al. 2025a. [Gemini: a family of highly capable multimodal models](#). *arXiv preprint arXiv:2312.11805*.

Google, Gemma Team, Aishwarya Kamath, Johan Ferret, Shreya Pathak, Nino Vieillard, Ramona Merhej, Sarah Perrin, Tatiana Matejovicova, Alexandre Ramé, Morgane Rivière, et al. 2025b. [Gemma 3 technical report](#). *arXiv preprint arXiv:2503.19786*.

Yash Goyal, Tejas Khot, Douglas Summers-Stay, Dhruv Batra, and Devi Parikh. 2017. Making the v in vqa matter: Elevating the role of image understanding in visual question answering. In *Proceedings of the IEEE conference on computer vision and pattern recognition*, pages 6904–6913.

Tianrui Guan, Fuxiao Liu, Xiyang Wu, Ruiqi Xian, Zongxia Li, Xiaoyu Liu, Xijun Wang, Lichang Chen, Furong Huang, Yaser Yacoob, et al. 2024. Hallusionbench: an advanced diagnostic suite for entangled language hallucination and visual illusion in large vision-language models. In *Proceedings of the IEEE/CVF Conference on Computer Vision and Pattern Recognition*, pages 14375–14385.

Stefan Heindorf, Yan Scholten, Henning Wachsmuth, Axel-Cyrille Ngonga Ngomo, and Martin Potthast. 2020. Causenet: Towards a causality graph extracted from the web. In *Proceedings of the 29th ACM international conference on information & knowledge management*, pages 3023–3030.

Donald D Hoffman and Whitman A Richards. 1987. Parts of recognition. In *Readings in Computer Vision*, pages 227–242. Elsevier.

Joy Hsu, Jiayuan Mao, Joshua B Tenenbaum, Noah D Goodman, and Jiajun Wu. 2024. What makes a maze look like a maze? *arXiv preprint arXiv:2409.08202*.

Drew A Hudson and Christopher D Manning. 2019. Gqa: A new dataset for real-world visual reasoning and compositional question answering. In *Proceedings of the IEEE/CVF conference on computer vision and pattern recognition*, pages 6700–6709.

Filip Ilievski, Alessandro Oltramari, Kaixin Ma, Bin Zhang, Deborah L McGuinness, and Pedro Szekely. 2021. Dimensions of common-sense knowledge. *Knowledge-Based Systems*, 229:107347.

Yifan Jiang, Kexuan Sun, Zhivar Sourati, Kian Ahrabian, Kaixin Ma, Filip Ilievski, Jay Pu-jara, et al. 2024. Marvel: Multidimensional abstraction and reasoning through visual evaluation and learning. *Advances in Neural Information Processing Systems*, 37:46567–46592.

Justin Johnson, Bharath Hariharan, Laurens Van Der Maaten, Li Fei-Fei, C Lawrence Zitnick, and Ross Girshick. 2017. Clevr: A diagnostic dataset for compositional language and elementary visual reasoning. In *Proceedings of the IEEE conference on computer vision and pattern recognition*, pages 2901–2910.

Koen Kraaijveld, Yifan Jiang, Kaixin Ma, and Filip Ilievski. 2025. Columbus: Evaluating cognitive lateral understanding through multiple-choice rebuses. In *Proceedings of the AAAI Conference on Artificial Intelligence*, volume 39, pages 4410–4418.

Ranjay Krishna, Yuke Zhu, Oliver Groth, Justin Johnson, Kenji Hata, Joshua Kravitz, Stephanie Chen, Yannis Kalantidis, Li-Jia Li, David A Shamma, et al. 2017. Visual genome: Connecting language and vision using crowdsourced dense image annotations. *International journal of computer vision*, 123:32–73.

Kenneth J Kurtz and Daniel C Silliman. 2021. Object understanding: Investigating the path from percept to meaning. *Acta Psychologica*, 216:103307.

Alan M Leslie and Stephanie Keeble. 1987. Do six-month-old infants perceive causality? *Cognition*, 25(3):265–288.

Junnan Li, Dongxu Li, Silvio Savarese, and Steven Hoi. 2023. Blip-2: Bootstrapping language-image pre-training with frozen image encoders and large language models. In *International conference on machine learning*, pages 19730–19742. PMLR.

Yian Li, Wentao Tian, Yang Jiao, Jingjing Chen, and Yu-Gang Jiang. 2024. Eyes can deceive: Benchmarking counterfactual reasoning abilities of multi-modal large language models. *arXiv e-prints*, pages arXiv–2404.

Bin Lin, Zhenyu Tang, Yang Ye, Jiaxi Cui, Bin Zhu, Peng Jin, Jinfa Huang, Junwu Zhang, Yatian Pang, Munan Ning, et al. 2024. Moe-llava: Mixture of experts for large vision-language models. *arXiv preprint arXiv:2401.15947*.

Jennifer S Lipton and Elizabeth S Spelke. 2004. Discrimination of large and small numerosities by human infants. *Infancy*, 5(3):271–290.

Pan Lu, Swaroop Mishra, Tanglin Xia, Liang Qiu, Kai-Wei Chang, Song-Chun Zhu, Oyvind Tafjord, Peter Clark, and Ashwin Kalyan. 2022. Learn to explain: Multimodal reasoning via thought chains for science question answering. *Advances in Neural Information Processing Systems*, 35:2507–2521.

Kenneth Marino, Mohammad Rastegari, Ali Farhadi, and Roozbeh Mottaghi. 2019. Ok-vqa: A visual question answering benchmark requiring external knowledge. In *Proceedings of the IEEE/cvf conference on computer vision and pattern recognition*, pages 3195–3204.

Minesh Mathew, Dimosthenis Karatzas, and CV Jawahar. 2021. Docvqa: A dataset for vqa on document images. In *Proceedings of the IEEE/CVF winter conference on applications of computer vision*, pages 2200–2209.

Michael McCloskey, Allyson Washburn, and Linda Felch. 1983. Intuitive physics: the straight-down belief and its origin. *Journal of Experimental Psychology: Learning, Memory, and Cognition*, 9(4):636.

George A Miller. 1995. Wordnet: a lexical database for english. *Communications of the ACM*, 38(11):39–41.

Daniel Mirman, Jon-Frederick Landrigan, and Allison E Britt. 2017. Taxonomic and thematic semantic systems. *Psychological bulletin*, 143(5):499.

OpenAI, Aaron Hurst, Adam Lerer, Adam P Goucher, Adam Perelman, Aditya Ramesh, Aidan Clark, AJ Ostrow, Akila Welihinda, Alan Hayes, Alec Radford, et al. 2024. Gpt-4o system card. *arXiv preprint arXiv:2410.21276*.

Ehsan Qasemi, Filip Ilievski, Muhao Chen, and Pedro Szekely. 2022. PaCo: Preconditions attributed to commonsense knowledge. In *Findings of the Association for Computational Linguistics: EMNLP 2022*, pages 6781–6796, Abu Dhabi, United Arab Emirates. Association for Computational Linguistics.

Nils Reimers and Iryna Gurevych. 2019. Sentence-bert: Sentence embeddings using siamese bert-networks. In *Proceedings of the 2019 Conference on Empirical Methods in Natural Language Processing*. Association for Computational Linguistics.

Amanpreet Singh, Vivek Natarajan, Meet Shah, Yu Jiang, Xinlei Chen, Dhruv Batra, Devi Parikh, and Marcus Rohrbach. 2019. Towards vqa models that can read. In *Proceedings of the IEEE/CVF conference on computer vision and pattern recognition*, pages 8317–8326.

Robyn Speer, Joshua Chin, and Catherine Havasi. 2017. Conceptnet 5.5: An open multilingual graph of general knowledge. In *Proceedings of the AAAI conference on artificial intelligence*, volume 31.

Elizabeth S Spelke and Katherine D Kinzler. 2007. Core knowledge. *Developmental science*, 10(1):89–96.

Chinthani Sugandhika, Chen Li, Deepu Rajan, and Basura Fernando. 2025. Situational scene graph for structured human-centric situation understanding. In *2025 IEEE/CVF Winter Conference on Applications of Computer Vision (WACV)*, pages 9215–9225. IEEE.

Niket Tandon, Gerard de Melo, and Gerhard Weikum. 2017. WebChild 2.0 : Fine-grained commonsense knowledge distillation. In *Proceedings of ACL 2017, System Demonstrations*, pages 115–120, Vancouver, Canada. Association for Computational Linguistics.

Yufei Tian, Abhilasha Ravichander, Lianhui Qin, Ronan Le Bras, Raja Marjieh, Nanyun Peng, Yejin Choi, Thomas L. Griffiths, and Faeze Brahman. 2025. Macgyver: Are large language models creative problem solvers?

Shengbang Tong, Zhuang Liu, Yuexiang Zhai, Yi Ma, Yann LeCun, and Saining Xie. 2024. Eyes wide shut? exploring the visual shortcomings of multimodal llms. In *Proceedings of the IEEE/CVF Conference on Computer Vision and Pattern Recognition*, pages 9568–9578.

Alexander Trott, Caiming Xiong, and Richard Socher. 2018. Interpretable counting for visual question answering.

Yi Ru Wang, Jiafei Duan, Dieter Fox, and Siddhartha Srinivasa. 2023. Newton: Are large language models capable of physical reasoning? *arXiv preprint arXiv:2310.07018*.

Zihao Wang and Lei Wu. 2023. Theoretical analysis of the inductive biases in deep convolutional networks. *Advances in Neural Information Processing Systems*, 36:74289–74338.

Li Xu, He Huang, and Jun Liu. 2021. Sutd-trafficqa: A question answering benchmark and an efficient network for video reasoning over traffic events. In *Proceedings of the IEEE/CVF*

conference on computer vision and pattern recognition, pages 9878–9888.

Wenhai Yu, Meng Jiang, Peter Clark, and Ashish Sabharwal. 2023. Ifqa: A dataset for open-domain question answering under counterfactual presuppositions. *arXiv preprint arXiv:2305.14010*.

Yuanyuan Yuan, Shuai Wang, Mingyue Jiang, and Tsong Yueh Chen. 2021. Perception matters: Detecting perception failures of vqa models using metamorphic testing. In *Proceedings of the IEEE/CVF Conference on Computer Vision and Pattern Recognition*, pages 16908–16917.

Jiarui Zhang, Jinyi Hu, Mahyar Khayatkhoei, Filip Ilievski, and Maosong Sun. 2024a. Exploring perceptual limitation of multimodal large language models. *arXiv preprint arXiv:2402.07384*.

Jiarui Zhang, Mahyar Khayatkhoei, Prateek Chhikara, and Filip Ilievski. 2025. Mllms know where to look: Training-free perception of small visual details with multimodal llms. *ICLR*.

Letian Zhang, Xiaotong Zhai, Zhongkai Zhao, Yongshuo Zong, Xin Wen, and Bingchen Zhao. 2024b. What if the tv was off? examining counterfactual reasoning abilities of multimodal language models. In *Proceedings of the IEEE/CVF Conference on Computer Vision and Pattern Recognition*, pages 21853–21862.

Susan Zhang, Stephen Roller, Naman Goyal, Mikel Artetxe, Moya Chen, Shuhui Chen, Christopher Dewan, Mona Diab, Xian Li, Xi Victoria Lin, et al. 2022. Opt: Open pre-trained transformer language models. *arXiv preprint arXiv:2205.01068*.

Jinguo Zhu, Weiyun Wang, Zhe Chen, Zhaoyang Liu, Shenglong Ye, Lixin Gu, Hao Tian, Yuchen Duan, Weijie Su, Jie Shao, et al. 2025. **Internvl3: Exploring advanced training and test-time recipes for open-source multimodal models.** *arXiv preprint arXiv:2504.10479*.

A Appendix: Technical Details

A.1 Prompt Strategies

A.1.1 Question Generation

We pass a standard prompt template to any of the three MLLMs: GPT-4o, Claude 3.7 Sonnet, and Gemini 2.0 Flash to generate questions, which are then used to inspire humans to generate new questions manually. The template is as follows:

{IMG} Generate three questions per prompt for this image with answers for each prompt. Prompt 1 deals with physical/taxonomic properties; prompt 2 deals with functional/relational properties; and prompt 3 deals with counterfactual reasoning. All need to be counting questions; be creative. You do not need to stick to the same questions.

A.1.2 Output Formatting

Table 4 displays the prompt templates used on instruction-tuned and non-instruction-tuned models to extract outputs in a specific format. Instruction-based models are also asked for a list of objects detected and considered for the count, which is currently not directly evaluated.

A.1.3 AI-Generated images

Table 5 shows the prompt examples used while generating AI-based images for different image domains.

A.2 Image Domains

During image collection (Figure 2), to direct our search, we made use of image domains inspired by the tags used in curating the MacGyver dataset (Tian et al., 2025). The three broad categories in this dataset are: indoors/household (e.g., kitchen), neutral (e.g., garage), and outdoors (e.g., zoo). Table 6 shows the list of 26 unique image domains used for the curation of OPTICS. The process of selecting a domain was influenced by the chance of a particular domain having a greater expected variety of objects. The domain tags used for the MacGyver dataset were plentiful, out of which 15 were in common, namely: bedroom, kitchen, library, meeting room, gym, wardrobe, garage, classroom, beach cleanup, camping, construction, gardening, zoo, park, and farm. The remaining 11 tags resulted from our exploration.

A.3 Benchmark Examples

A.3.1 Image Types

Figure 8 shows additional examples from OPTICS-CNT for three image types: Photographic, Animated, and AI-generated.

A.3.2 Object Property Dimensions

Table 7 shows examples of questions present per object property dimension.

A.3.3 Reasoning Complexity

Table 8 shows examples of the questions asked at the different reasoning levels. Direct recognition has questions from the physical and taxonomical object property dimensions; property inference has questions from the functional and relational dimensions; and counterfactual reasoning has questions from any of the four property dimensions.

A.3.4 OPTICS-CMP

Figure 9 shows an example from OPTICS-CMP where we merge two images from OPTICS-CNT into a single image. Figure 10 visualizes the sample distribution across count-difference levels and question categories.

A.4 Ground Truth Distribution

For the total number of 1,080 questions, the ground truth distribution for all the counts ranging from 0 to 10 is shown in Figure 11.

A.5 Examples of Model Errors

OPTICS requires models to have good low-level perception and the ability to perform fine-grained analysis. A case study on the errors models typically make is visually depicted using an image of *photographic* type. Figure 12 shows an instance from OPTICS-CNT, with the ground truth values provided after the question in the yellow cell and the depiction of object counts through green bounding boxes. The bounding boxes are manually annotated on the images using Canva.² To showcase the output of the model, we consider the open-source model, Gemma 3 (27B), for this study. Figure 13 displays the model’s predicted values and the probable object selection, with green (correct) and red (incorrect) bounding boxes based on detailed reasoning explicitly requested for this image.

²<https://www.canva.com/>

Category	Prompt Template
Non-Instruction-tuned models	<p><i>{IMG}</i></p> <p>Question: <i>{question}</i> Provide only the total number. Answer:</p>
Instruction-tuned models	<p><i>{IMG}</i></p> <p><i>{question}</i> Your response MUST be in the following format and nothing else: <NUMBER> [<OBJECT1>, <OBJECT2>, <OBJECT3>, ...]</p>

Table 4: Prompt template used to extract output in a specific format from the model for non-instruction-tuned and instruction-tuned models. *{IMG}* and *{question}* are the placeholders for the image and question, respectively.

Image Domain	Prompt Example
Campsite settings (Outdoors)	<p>Create image Generate a photorealistic dusk campsite scene with 5 tents, a few of them illuminated from within, a controlled campfire with 3 people sitting on logs around it and a dog sleeping nearby, hiking backpacks leaning against a nearby tree, a lantern hanging from a branch, and stars beginning to appear in the darkening sky. Include a mountain silhouette in the background. Strictly keep the count of total objects in the image to a maximum of 10.</p>
Gym (Indoors/Household)	<p>Create image Generate a photorealistic image of a gym scene with sports equipment. Let the gym contain 3 treadmills, 2 elliptical machines, a few kettlebells on the floor, 2 resistance bands hanging on the wall, and a bench press rack. Let it be a realistic setting with 2 humans working out, one person on the treadmill and another person on the elliptical machine. The gym can have a clock and TV hanging on the wall somewhere showing a workout video. Include large windows with natural light and a small plant in the corner. Strictly keep count of total objects in the image to a maximum of 10.</p>
Beach cleanup (Outdoors)	<p>Generate a photorealistic image of a beach cleanup scene with 4 volunteers in bright t-shirts collecting trash at sunset in the backdrop. Let the trash include these objects: 5 glass bottles, 6 trash bags (one in each hand of a volunteer and 2 placed near the ground), a collection bin, reusable gloves, and garbage pickers. Let it be a realistic setting, having the ocean with gentle waves in the background. Strictly keep the count of total objects in the image to a maximum of 10.</p>
Garage (Neutral)	<p>Create image Create a photorealistic image of a vehicle garage scene during a vehicle maintenance session. Show 3 cars, one car on a hydraulic lift with its hood open, 2-3 essential tools spread on a workbench, an oil change in progress, spare parts in organised containers, and a service manual. Let the setting be realistic with ceiling lights for the garage, let the car being serviced be in good condition, and let the other two cars in the background be scrap and old, which need to be rebuilt with loose tires leaning next to them. Let one person work on the car that is being serviced and the other person in the backdrop next to the other 2 cars. Strictly keep count of total objects in the image to a maximum of 10.</p>
Kitchen (Indoors/Household)	<p>Create image Generate an image of a kitchen countertop during the preparation of a complex dish. Show fresh ingredients arranged in 3 small ceramic bowls, a wooden cutting board with chopped herbs, a professional knife set, a simmering pot on the stove, a recipe book, a glass filled with water, and 2 people collaborating on the cooking. Include details like steam, a kitchen sink next to the stove, and ambient kitchen lighting. Let it be a realistic setting. Strictly keep the count of total objects in the image to a maximum of 10.</p>

Table 5: Prompt examples used to generate AI images across different domains, along with corresponding tags (shown in brackets) used in constructing the MacGyver dataset. Prompts with the **Create Image** tool are generated using GPT-4o, while those without it are created with Grok 3.

Indoors/Household	Neutral	Outdoors
bedroom	tools	beach cleanup
home setup	tech	camping
kitchen	garage	construction
library	classroom	gardening
laboratory		biking
meeting room		market
gym		zoo
salon		urban
wardrobe		park
		picnic
		farm
		driveway
		bustop

Table 6: The 15 domains (i.e., locations and activities) taken from the MacGyver dataset (Tian et al., 2025), extended with 11 of our own, for a total of 26 unique image domains. They are broadly divided into Indoors/Household, Neutral, and Outdoors.

For the first question, the model outputs 5, as it misses the sparrow that is partially occluded but still visible to the human eye. In the second question, the model outputs 6, as it tends to over-count the row of chairs due to the challenging angle at which the picture is captured. In the final question, the model outputs 2, reasoning that there are three birds (excluding the partially visible one) on the right sitting together on one railing, leaving two birds on the left. But in the ground truth, the bird positioned on the extreme right is sitting on a different metal frame. Based on the model’s answer to the first question, its reasoning is consistent with the third question’s answer.

The model fails to detect objects that are partially hidden, indicating weak low-level perception. It misinterprets perspective and geometric layout and struggles to distinguish objects that are closely clustered together. Despite the incorrect answers, the model’s internal reasoning is logically consistent. This study highlights the importance of evaluating not only the final count, but also the quality of visual grounding and traceability of reasoning for tasks like those in OPTICS, providing potential for future work.

B Appendix: Complementary Results

B.1 Inductive Bias

The BLIP2 model series consistently defaults to specific output values, suggesting the presence of inductive bias in the models. The OPT 2.7B vari-

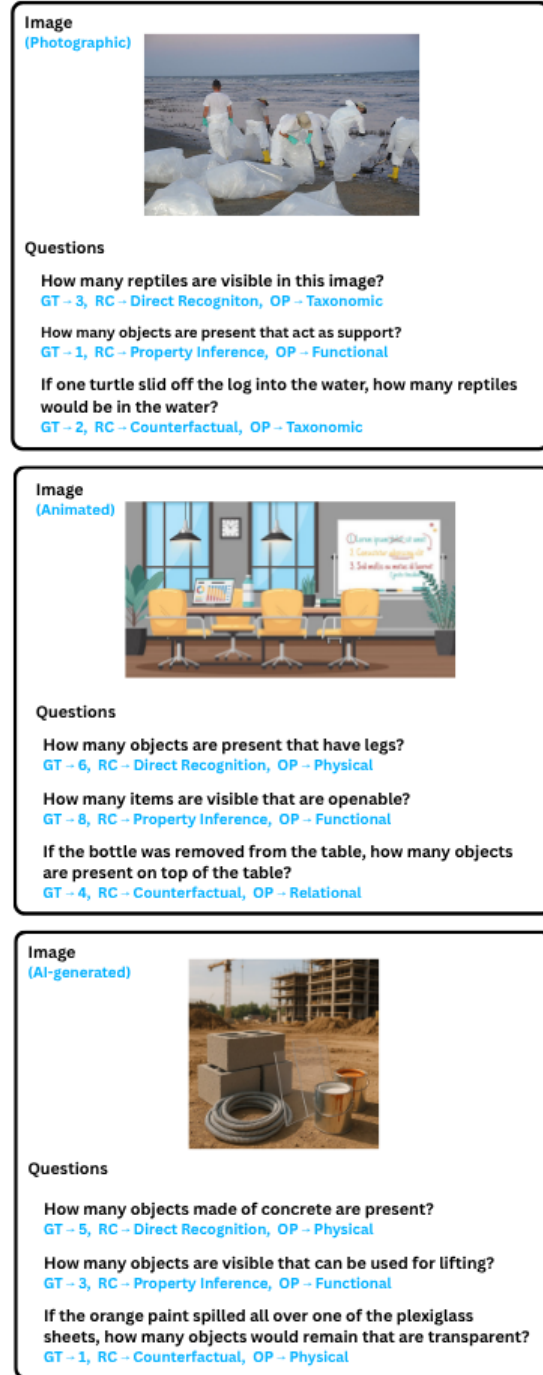


Figure 8: Examples from OPTICS-CNT, for three image types: Photographic (top), Animated (middle), and AI-generated (bottom). Text highlighted in blue is information stored in the benchmark and not passed to the model during evaluation. GT stands for ground truth, RC for reasoning complexity, and OP for object properties.

ant goes for the count 1, the OPT 6.7B variant produces either 1 or 3 as the output, and the Flan T5 xxL gives an output of 0 or no value or an an-

Dimensions	Question Examples
Physical	<p>How many objects made of wood are present?</p> <p>How many objects are present that are transparent?</p> <p>How many objects in the background are present that have legs?</p>
Taxonomic	<p>How many mammals are visible in the image?</p> <p>How many furniture items are present in the room?</p> <p>How many tools are visible in the image?</p>
Functional	<p>How many objects with the primary purpose of illumination can be seen?</p> <p>Count the number of breakable items?</p> <p>Count the number of items that are battery powered?</p>
Relational	<p>How many objects are visible that are attached to the wall or ceiling?</p> <p>How many reptilian couples, at maximum, are present?</p>

Table 7: Question examples for the different object property dimensions: physical, taxonomic, functional, and relational.

OPTICS-CNT



Question: If the two bedside lamps were removed, how many objects are present that need electricity?
Answer: 2



Question: If the lamp were removed, how many objects would need electricity?
Answer: 0

OPTICS-CMP



Question: Let A be the answer to "If the two bedside lamps were removed, how many objects are present that need electricity?" for the left image.
Let B be the answer to "If the lamp were removed, how many objects would need electricity?" for the right image. Which is greater, A or B?
Answer: A

Figure 9: Example from OPTICS-CMP with a count difference of 2.

swer not abiding by the required format (numeric value), resulting in a final output of 0 set according

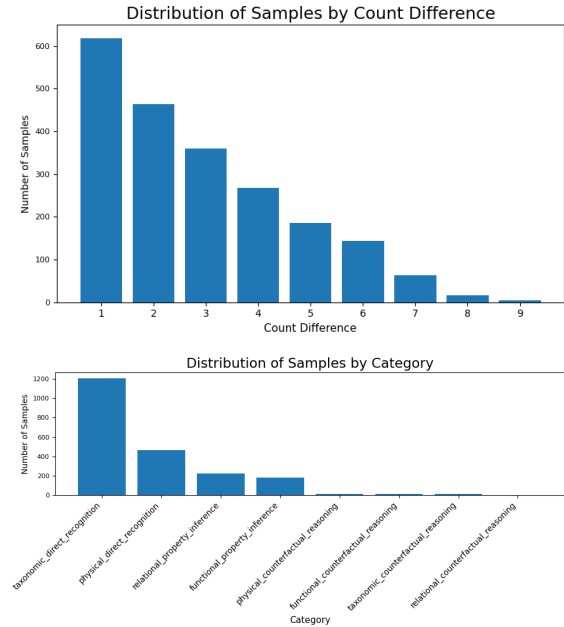


Figure 10: Sample Distribution of OPTICS-CMP.

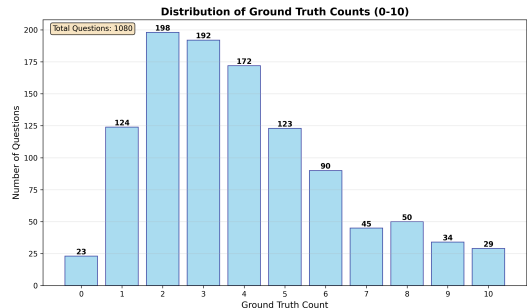


Figure 11: Ground Truth distribution for all counts ranging from 0 to 10.

to our answer extraction method. The frequency distribution of these outputs is shown in Figure 14. We tried adjusting prompts and decoding parameters, such as the number of maximum new tokens, but none helped mitigate the issue, highlighting the potential inductive biases present in models (Wang and Wu, 2023; Kraaijveld et al., 2025).

B.2 Cumulative Accuracies with Tolerance

The soft off-by-1 accuracy metric, which has a baseline of 25.62%, reveals relatively better improvements (47.16% gap with the best model) among the larger instruction-tuned models. Even though the models predictions are often nearly correct, this metric highlights the difficulty in precise numeric predictions by VLMs. The cumulative accuracy for tolerance values 0, 1, and 2 is

Complexity	Dimension	Question Example
Direct Recognition	physical taxonomic	How many objects made of wood are present? How many mammals are visible in the image?
Property Inference	functional relational	Count the number of breakable items? How many objects are visible that are attached to the wall or ceiling?
Counterfactual	physical	If one of the metal objects were replaced by a wooden object, how many wooden objects would be there in the image?
	taxonomic	If one person leaves the cleaning group, how many mammals would remain?
	functional	If the two bedside lamps were removed, how many objects are present that need electricity?
	relational	If the signages were removed, how many objects would be present that hang from the ceiling?

Table 8: Question examples for the different reasoning complexity levels that is direct recognition, property inference, and counterfactual.

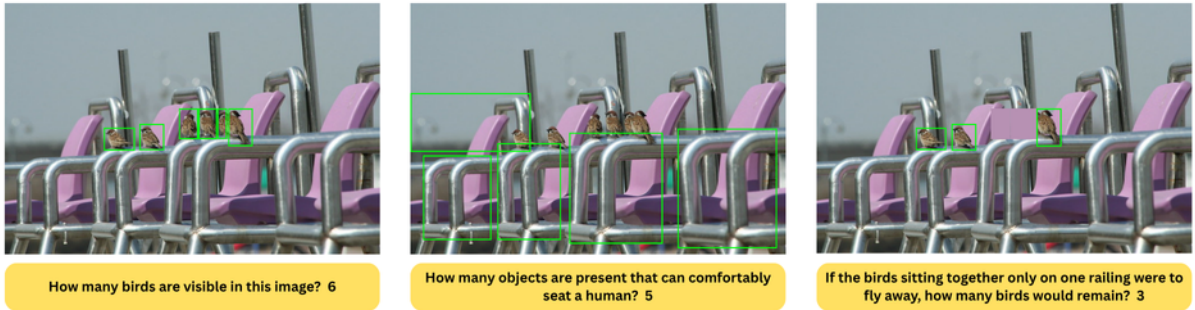


Figure 12: Questions follow the reasoning complexity order, direct recognition to counterfactual (left to right) for a photographic image with the ground truth values and the object counts visually depicted by green bounding boxes.

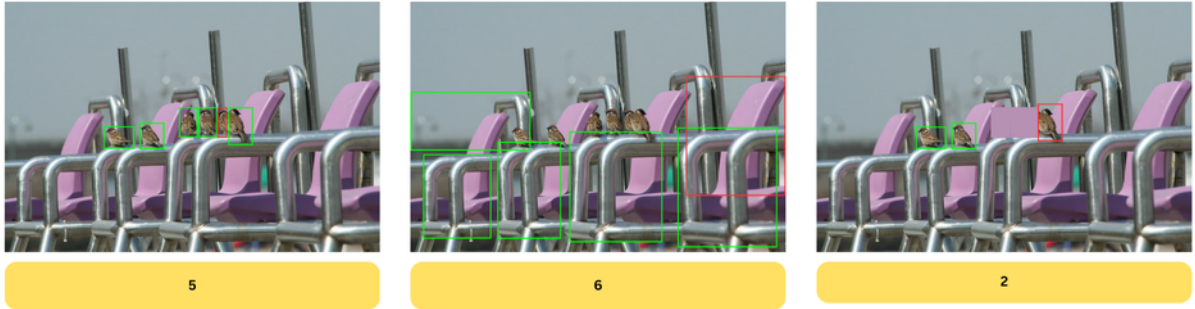


Figure 13: Gemma 3 model output values and the visual depiction of possible **correct** and **incorrect** detections.

shown in Figure 15 for the top-performing models in their categories and the average of the human evaluators.

B.3 OPTICS-CMP results

Table 9 shows the results for seven instruction-tuned models evaluated on OPTICS-CMP.

B.4 Error Analysis of Humans and Qwen

The raw results of this analysis are provided in Table 10.

B.5 Visual Genome-based Dataset Curation

Figure 16 shows two examples of question-answer pairs generated automatically from Visual Genome. We pose the following question: *Can densely annotated datasets be used to scale up*

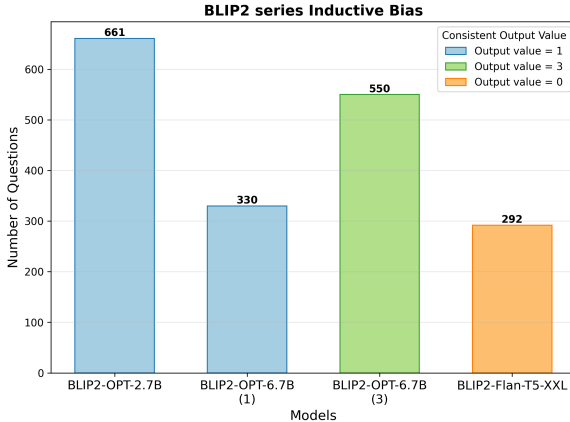


Figure 14: BLIP2 model series inductive bias plot, consistently defaulting to specific output values.

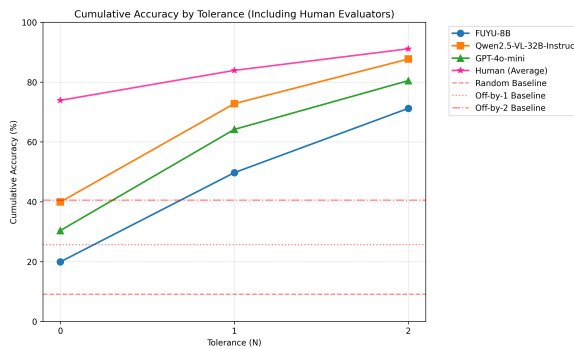


Figure 15: Cumulative accuracies for tolerance levels 0, 1, and 2. The top-performing models from the following categories are shown: open-source non-instruction VLM (Fuyu-8B), open-source instruction VLM (Qwen2.5-VL-32B-Instruct), closed-source VLM (GPT-4o mini), the human evaluators average and the random chance baselines for tolerance levels 0 (9.09%), 1 (25.62%), and 2 (40.50%).

OPTICS-CNT automatically? Visual Genome (VG) (Krishna et al., 2017) is a popular dataset with high-quality structured connections between image regions, language descriptions, and WordNet (Miller, 1995) synsets. To investigate whether the annotations of VG can support the generation of large-scale instantiations of OPTICS, we devised a procedure that generates taxonomic questions by manipulating the WordNet synsets. This experiment exposed three limitations: lack of contextualization of classes (e.g., kitchen utensil instead of a bowl in Figure 16-left), incorrect questions or answers (e.g., about uncountable objects like grass in Figure 16-right), and classes in the WordNet hierarchy that are not overly specific (e.g., derby horse race) or generic (e.g., entity). Thus, while every image in VG enables many tax-

Model	Micro Acc (\uparrow)	Macro Acc (\uparrow)
Qwen2.5 (3B)	55.14	56.30
Qwen2.5 (7B)	57.54	58.10
Qwen2.5 (32B)	68.33	72.39
InternVL3 (8B)	<u>62.02</u>	64.35
InternVL3 (14B)	46.84	64.19
Gemma3 (27B)	54.52	<u>64.48</u>
GPT-4o mini	60.34	64.45
<i>Model average</i>	57.81	63.46

Table 9: Zero-shot results on OPTICS-CMP. The micro accuracy and macro accuracy (average across count differences (1-9)) are reported. The highest and second-highest model results are highlighted in **bold** and underlined, respectively. (\uparrow) indicates that higher values are better.

onomic questions to be created, it remains challenging to automatically distinguish high- from low-quality question-answer pairs. More fundamentally, creating question-answer pairs for other object properties (e.g., functional) and reasoning types (e.g., counterfactual) is hindered by the absence of annotation. While LLMs can be employed to generate questions for these categories, we established that these questions and answers are often incorrect or ambiguous (e.g., suggesting that buildings, doors, and windows can all provide shelter). In conclusion, we find that densely annotated image datasets remain insufficient to generate high-quality large-scale versions of OPTICS. Yet, they could potentially be used to speed up human annotation by providing an initial set of samples or for distant supervision of VQA models.

	Semantic ambiguity	Visual ambiguity	Perception errors	Unnatural errors
Human	16	3	9	0
Qwen2.5 (32B)	8	1	8	9

Table 10: Results from analyzing the errors made by humans and the model.

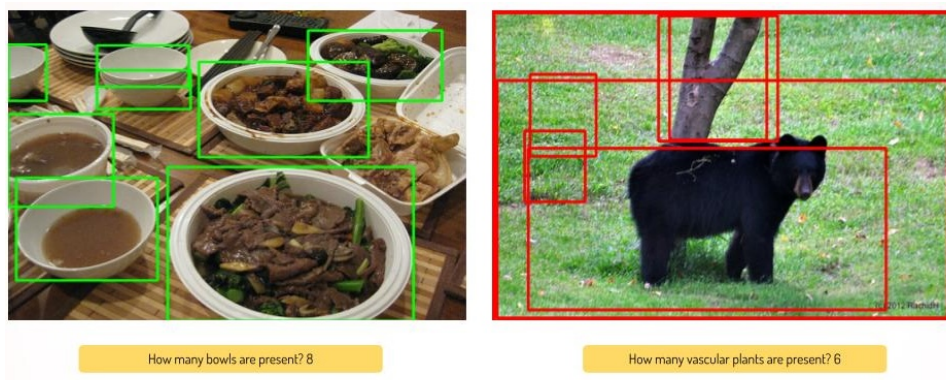


Figure 16: **Left:** A successful example of a question generated using Visual Genome. **Right:** An unsuccessful example, where multiple objects are assigned to a single tree and a single patch of grass, leading to an incorrect answer.